International Journal of Steel Structures (2020) 20(5):1783–1795
https://doi.org/10.1007/s13296-020-00410-9

Online ISSN 2093-6311
Print ISSN 1598-2351

Parameters Effect on Predicting Fire Resistance of Ultra-high Strength Concrete Filled Protected Square Steel Tubular Columns

Xiao Lyu[1,2] · Gan-Ping Shu[3,4] · Er-Feng Du[3,4]

Received: 1 July 2017 / Accepted: 8 September 2020 / Published online: 14 September 2020

Abstract

Ultra-high strength concrete (UHSC) with compressive strength greater than 100 MPa at room temperature has been developed for concrete filled square steel tubular column for use in high-rise buildings. The fire resistance of UHSC filled protected square steel tubular columns exposed to the standard ISO fire is investigated in this paper. For this purpose, numerical heat transfer analysis and nonlinear thermal stress analysis were conducted by taking into account the existing material properties, such as the thermal and mechanical properties of UHSC and high strength steel. The numerical analyses were carried out and the results were validated against the test results in terms of heat distribution and mechanical behavior. Comparison with the test results showed a reasonable agreement with finite element results in terms of temperature field prediction and load displacement behavior during the fire. Finally, based on the validated finite element model, the effects of fire protection thickness, load ratio, the strengths of concrete and steel, steel contribution ratio, and relative slenderness ratio on the fire resistance of UHSC filled square steel tubular columns were carried out and discussed.

Keywords Thermal analysis · Constant axial load · Fire resistance · Protected square steel tubular column · Ultra-high strength concrete · Mechanical properties

1 Introduction

The use of composite construction has become more widespread in recent decades. Depending on several advantages such as high load-bearing capacity, inherent ductility and toughness, concrete-filled steel tubular columns are commonly used in high-rise buildings and bridges. The main benefit of using concrete filled tubular columns is the increase of load bearing capacity without the need of additional formwork. Their fire resistance can also be further enhanced with infilled concrete (Chung et al. 2009; Rush et al. 2012; Shu and Lv 2013). This is likely due to the fact that concrete core traps the heat inside the steel tube. In other words, the concrete core acts as heat sink which reduces the temperature of the steel tube when the concrete filled steel tube is subjected to fire (Xiao et al. 2016; Jamaluddin et al. 2013; Qu et al. 2015). Fire resistance is defined as the duration during which a structural member exhibits resistance with respect to structural integrity, stability, and temperature transmission under fire conditions (Hassanein et al. 2015; Fong et al. 2011). In high-rise buildings, fire resistance is a critical design consideration for columns since fire represents one of the most severe conditions that may be encountered during the life time of a building (Mao and Kodur 2011).

Studies on the fire resistance of square steel tubular columns infilled with normal and high strength concrete have been carried out by many researchers (Wang and Young 2013; Han et al. 2003; Chung et al. 2013; Lyu et al. 2018). Recent research focuses on the use of ultra-high strength concrete (UHSC) as infilling material to form concrete filled tubular members (CFTs) (Lee et al. 2012; Choe et al. 2015; Shin et al. 2015). Steel tubular members infilled with UHSC with compressive strength up to 180 N/mm^2 provide higher

✉ Gan-Ping Shu
sgp0818@vip.sina.com

1 School of Civil Engineering, Shandong Jianzhu University, Jinan 250101, China

2 Key Laboratory of Building Structural Retrofitting and Underground Space Engineering (Shandong Jianzhu University), Ministry of Education, Jinan 250101, China

3 School of Civil Engineering, Southeast University, Nanjing 210096, China

4 Key Laboratory of C & PC Structures, Ministry of Education, Southeast University, Nanjing 210096, China

compression resistance and, therefore, smaller column size. Liew et al. (2014) have investigated the behavior of such columns in both ambient temperature and fire situations.

Square CFT columns without fire protection were used in the actual construction of the parking garage of Samsung Electronics in February 2007. This was the first time the type of construction was used in Korea (Park et al. 2008).

High strength materials have been found to be attractive alternatives to normal strength materials for high-rise construction. The use of high strength materials is feasible for columns in high rise buildings. This is because the higher the material strength, the smaller the member size is required to resist the same design load. As ultra-high strength concrete is used in concrete filled tubes, the confinement provided by the steel tube can improve the post-peak ductility of the ultra-high strength concrete depending on the steel contribution ratio as observed by Liew et al. (2015) in the experimental studies. The aim of this paper is to attempt to propose a numerical model for temperature field calculations and thermal–mechanical analyses of UHSCFST columns and learn various parametric effects on fire resistance.

In the numerical model, the fire resistance of UHSCFST columns is calculated in various steps, consisting of temperature calculation of the fire to which the column is exposed, the temperature distribution across the cross-section of column, the deformations during exposure to fire and, finally, the fire resistance. This paper presents the nonlinear finite element analysis model to simulate the fire performance of UHSCFST columns exposed to the standard fire condition. The composite action between the steel and concrete has been considered in the numerical model. The column is subjected to constant axial compression followed by heating under the standard ISO fire until failure. The analysis is considered of the influences of temperature on the strength and modulus of the UHSC material based on the test data from an existing literature (Xiong 2013). The accuracy of the numerical model is established by comparing the numerical results with test results. Finally, parametric studies are carried out to evaluate the effects of fire protection thickness, load ratio, strengths of concrete and steel, steel contribution ratio and relative slenderness ratio on fire resistance of protected square steel tubular members infilled with UHSC. By varying these parameters, an economical design, that satisfies the fire resistance requirements for structures, can be determined.

2 Temperature Calculation of Concrete Filled Square Steel Tubular Columns

The specimens for the analyses are taken from available reference (Xiong 2013). All the specimens are 3.81 m long from end plate to end plate with 3 m long exposed to fire in the furnace, and the details are shown in Table 1 and Fig. 1a, b. The prediction of the temperature field of UHSCFST column is based on the fire temperature in the furnace.

The fire resistance of ultra-high strength concrete filled square tubular column depends on the fire temperature to which the column is exposed, the temperature field in the column, the strength of the materials at elevated temperature and the member deformations during the fire exposure.

The two-dimensional heat flow problem is modeled mathematically based on Fourier law of heat transfer. A statement of the heat conduction balance equation is given below,

$$\frac{\partial T}{\partial t} = \frac{\lambda}{c \cdot \rho}\left[\frac{\partial}{\partial x}\left(\frac{\partial T}{\partial x}\right) + \frac{\partial}{\partial y}\left(\frac{\partial T}{\partial y}\right)\right] + \frac{Q}{c \cdot \rho} \tag{1}$$

where c material specific heat (J/kg K), ρ material density (kg/m^3), λ material thermal conductivity (W/m K).

By assuming that furnace fire is the fire source, the heat convection and heat radiation is calculated as follows,

$$q = \alpha_c(T_f - T_s) + \varepsilon\sigma\left[(T_f + 273)^4 - (T_s + 273)^4\right] \tag{2}$$

where $\alpha_c = 25$ W/m^2 K is the convection coefficient, $\varepsilon = 0.5$ is the resultant emissivity of the furnace and the exposed refractory surface, $\sigma = 5.67 \times 10^{-8}$ W/(m^2 K^4) is

Table 1 Details of the UHSCFST columns

Specimen	Diameter × thickness D (mm) × t_s (mm)	Steel yield strength f_y (MPa)	Modulus of elasticity E_s (GPa)	Concrete cylinder strength f_c (MPa)	t_p^* (mm)	δ^*	$\overline{\lambda}^*$
USZ-1	200 × 12	785	211	174	8.0	0.57	0.58
USZ-2	200 × 12			173	11.5	0.57	0.58
USZ-3	200 × 12			170	9.1	0.57	0.57
USZ-4	200 × 12			166	8.8	0.58	0.57
USZ-5	200 × 12			166	9.5	0.58	0.57

t_p is thickness of fire protection. $\delta = A_s f_y/(A_s f_y + A_c f_c)$ is the steel contribution ratio. $\overline{\lambda}$ is the relative slenderness.

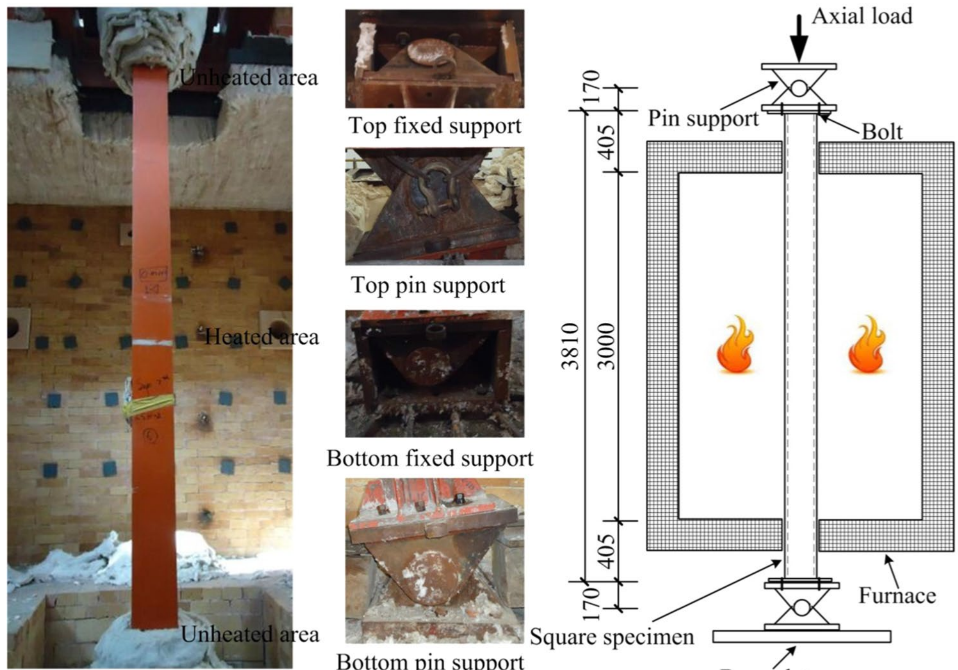

(a) Square specimen in furnace (Xiong' s test) **(b)** Schematic of the experiment setup

Fig. 1 Boundary condition for column specimen in test (Xiong 2013)

the Stefan–Boltzmann constant (ECCS 1988), T_s is average surface temperature, T_f is temperature of furnace fire.

Using the temperature-dependent thermal properties of the concrete and steel, the temperature history of the column can be obtained by solving the heat balance equation (ISO 834-1 1999). A two-dimensional nonlinear thermal analysis model for the UHSCFST column exposed to a fire on four sides is considered, with the assumption that no heat is flowing along the longitudinal axis (Yu et al. 2010; Dai and Lam 2012). The finite element simulations for both the heat transfer and structural analyses are conducted using the general finite element analysis package ABAQUS.

2.1 Thermal Properties of the Ultra-high Strength Concrete (UHSC)

The thermal properties include the thermal conductivity, specific heat, thermal expansion, and the mass loss of the material at elevated temperatures. There are three material models of thermal properties which are often adopted for the heat transfer calculations. One is the Lie's thermal model (Lie 1992), the second one is the AIJ code model (AIJ 2008), and the third one is the Eurocode model. In this paper, the thermal model is based on the Eurocode model (Eurocode 2 2004; Eurocode 4 2005). Generally, the lower limit of thermal conductivity is used for normal strength concrete (NSC), while the upper limit is considered for high strength concrete (HSC) and ultra-high strength concrete (UHSC). The moisture content is assumed to be 3% for NSC and HSC, whereas it is ignored for UHSC (Xiong and Liew 2016).

2.2 Thermal Properties of the Fire Protection Material

In the fire tests reported in reference (Xiong 2013), the fire protection material was a mixture of Portland cement (40%), perlite (25%), vermiculite (20%) and water (15%) by weight. The thermal properties are assumed not to change with temperature. The thermal conductivity = 0.116 W/m K, specific heat = 1010 J/kg K and density = 305 kg/m^3 are adopted based on the test data.

2.3 Thermal Analysis of the Specimens

The initial ambient temperature is set as 20 °C. In the thermal analysis, 4-node shell element (DS4) is adopted to model the steel tube and 8-node brick element (DC3D8) for the concrete core and the fire protection with three layers along its thickness. The heat convection and radiation are considered as boundary conditions in the thermal analysis as shown in Fig. 2a–c. The height of specimen exposed to fire is 3.0 m, while the height of specimen is 3.81 m. The composite column is subjected to uniform heating (close to the ISO standard fire) from the surrounding air in the furnace during the entire heating process.

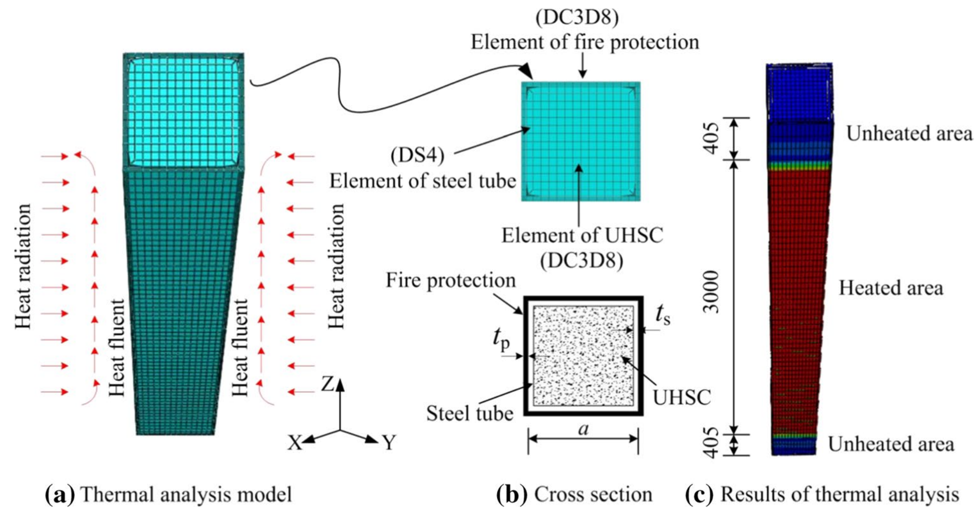

Fig. 2 Boundary conditions for temperature field and calculation results

2.4 Comparison Between the Predicted and Experimental Results

There are three measure points in the UHSCFST column. Point 1 is at the centre of column cross-section, Point 2 is at the position of $a/4$ (a is the edge length of square concrete core) and Point 3 is at the edge of the concrete core. The predicted temperatures based on the finite element analyses are compared with the measured temperatures from the tests, as shown in Fig. 3. The furnace temperature was measured and plotted in Fig. 3a–e.

For specimen USZ-1, the measured temperature at Point 1 and 2 compared well with the predicted results. The mean error between the predicted temperature and measured temperature is less than 3% for point 1, 4% for Point 2. For measured temperature at Point 3, with the temperature increasing, the value of the error becomes increasing. This is because that the thermocouple was damaged after 15 min during the experiment. The results of specimen USZ-2 and USZ-4 are similar to specimen USZ-1, the comparisons showed that the predicted temperatures were in reasonable agreement with the measured values, especially for Point 1 and 2. As shown in Fig. 3b, d, the mean errors between the predicted temperature and measured temperature for Points 1 and 2 are less than 5%, although the mean error is about 14% for Point 3. For specimens USZ-3 and USZ-5, the mean errors between the predicted temperature and measured temperature for Points 1, 2 are less than 5%, although the mean error is about 9% for Point 3.

3 Mechanical Properties at Elevated Temperature

3.1 Ultra-high Strength Concrete (UHSC)

There is limited information on the mechanical properties of UHSC at elevated temperature. Xiong (2013) conducted tests to evaluate the elastic modulus and compressive strength of the UHSC at elevated temperatures. In the tests, cylinder specimens with diameter = 100 mm and height = 200 mm were prepared. The specimens were heated in a furnace without pre-loading at a rate of 5 °C/min until the target temperature was reached. Dosage of 0.1% polypropylene in volume was added into UHSC in case of spalling during heating. The target temperatures ranged between 100 and 800 °C at an increment of 100 °C. Once the target temperature was reached, it was held for 4 h to ensure that the temperature was uniformly distributed inside the test specimen. Finally, the specimen was subjected to compression until failure with displacement rate 0.4 mm/min during loading. A typical stress–strain relationship of UHSC at elevated for specimen USZ-1 is shown in Fig. 4. The reduction factors of the elastic modulus and compressive strength for specimens are shown in Tables 2 and 3, respectively. The test data were fitted into the stress–strain models in Eurocode 2 (Eurocode 2 2004) as follows,

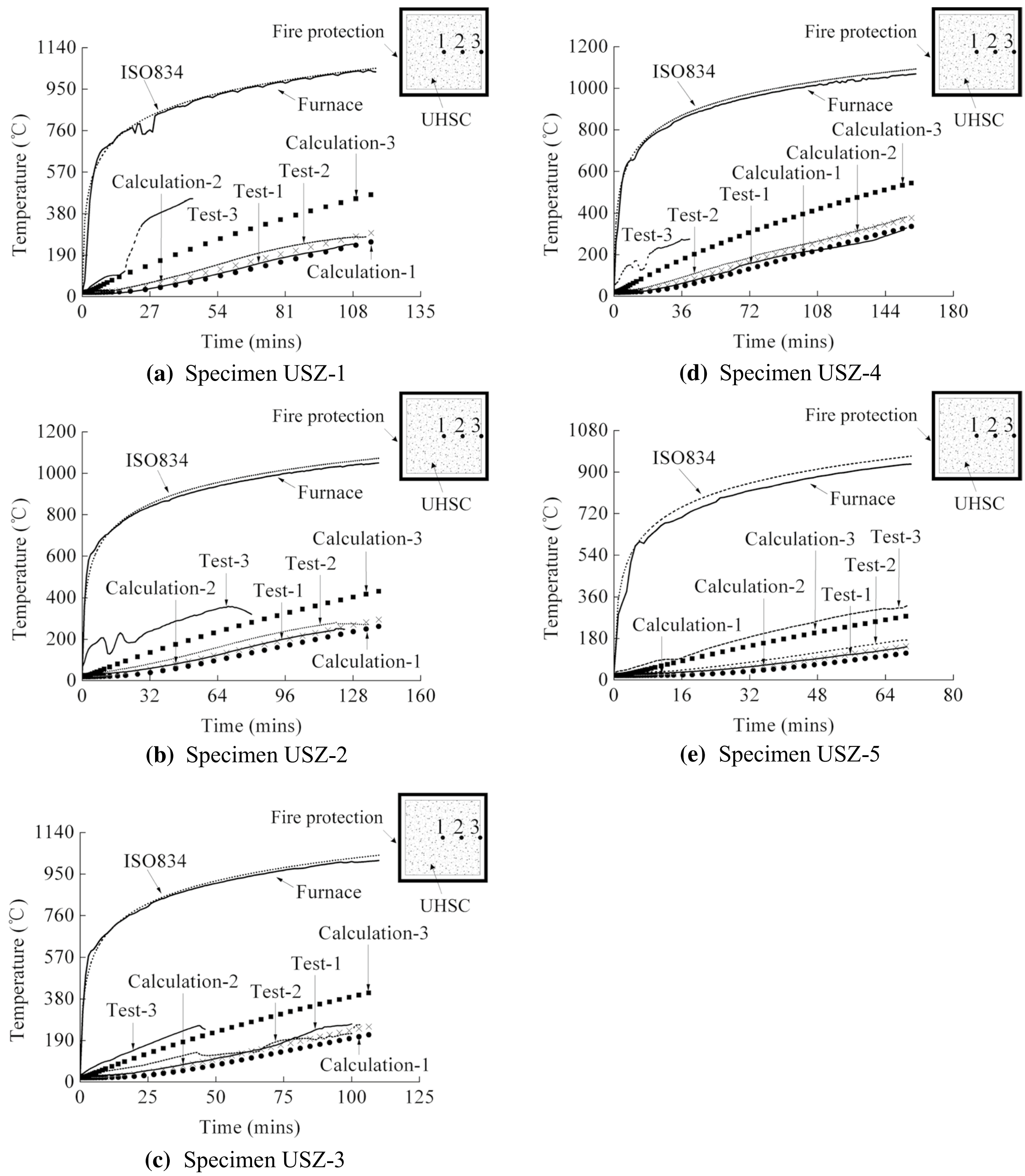

Fig. 3 Comparison between the predicted and measured temperatures for specimens USZ-1–5

$$\sigma = \frac{3\varepsilon f_{c,\theta}}{\varepsilon_{c1,\theta}\left[2+\left(\frac{\varepsilon}{\varepsilon_{c1,\theta}}\right)^{3}\right]} \quad 0 \le \varepsilon \le \varepsilon_{cu1,\theta} \tag{3}$$

where $f_{c,\theta}$ is the compressive strength, $\varepsilon_{c1,\theta}$ is the strain corresponding to $f_{c,\theta}$, $\varepsilon_{cu1,\theta}$ is the strain for defining range of the descending branch.

Spalling was not observed during heating of all specimens. As shown in Table 2, for the elastic modulus of UHSC at elevated temperature, an unusual deterioration and recovery were observed at the temperature range of 100–200 °C. For the compressive strength of UHSC at elevated temperature, an unusual deterioration was observed at the temperature 100 °C, which was shown in Table 3. However, with temperature increased range of 100–300 °C, the strength was partly recovered. At 800 °C, the strength was only about 30% of that at room temperature.

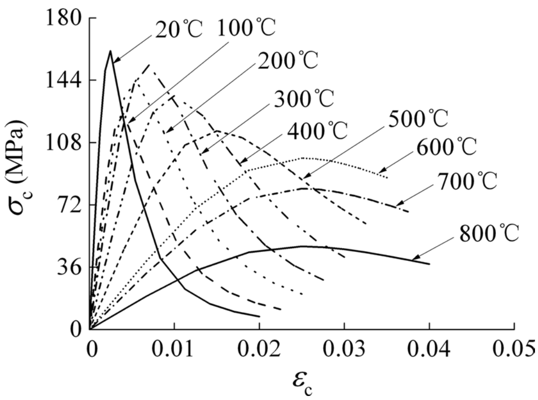

Fig. 4 Stress–strain relationship for UHSC of USZ-1 at various temperatures

As shown in Fig. 4, the peak stress decreases sharply at 100 °C and recovery was observed at the temperature range of 100–300 °C, which is the same as the compressive strength. The stress decreases sharply after the peak stress at temperature range of 20–300 °C, but it decreases gently at temperature range of 400–800 °C.

3.2 Steel

Eurocode 3 (Eurocode 3 2005) provides the equations to describe the elastic modulus and effective strength of steel at elevated temperature. The reduction factors of elastic modulus, yield strength and the relationship of stress and strain at elevated temperature given in Eurocode 3:1–2 (Eurocode 3 2005) are adopted for the numerical analysis.

4 Fire Resistance of UHSCFST Columns

4.1 Eurocode 4 Approach

According to the simplified method in Eurocode 4 (Eurocode 4 2005), the plastic resistance of the concrete filled square cross-section may be calculated as:

Table 2 Reduction of secant modulus for UHSC at elevated temperature

Temperature (°C)	USZ-1 (MPa)	USZ-2 (MPa)	USZ-3 (MPa)	USZ-4 (MPa)	USZ-5 (MPa)	Mean reduction
20	1.03×10^5	1.03×10^5	1.01×10^5	9.86×10^4	9.86×10^4	1.00
100	8.55×10^4	8.55×10^4	8.38×10^4	8.18×10^4	8.18×10^4	0.83
200	9.27×10^4	9.27×10^4	9.09×10^4	8.87×10^4	8.87×10^4	0.90
300	7.73×10^4	7.73×10^4	7.58×10^4	7.40×10^4	7.40×10^4	0.75
400	5.67×10^4	5.67×10^4	5.56×10^4	5.42×10^4	5.42×10^4	0.55
500	4.64×10^4	4.64×10^4	4.55×10^4	4.44×10^4	4.44×10^4	0.45
600	3.09×10^3	3.09×10^3	3.03×10^3	2.96×10^3	2.96×10^3	0.30
700	2.58×10^3	2.58×10^3	2.53×10^3	2.47×10^3	2.47×10^3	0.25
800	2.37×10^3	2.37×10^3	2.32×10^3	2.27×10^3	2.27×10^3	0.23

The data were obtained from Xiong's experiments

Table 3 Reduction of compressive strength for UHSC at elevated temperature

Temperature (°C)	USZ-1 (MPa)	USZ-2 (MPa)	USZ-3 (MPa)	USZ-4 (MPa)	USZ-5 (MPa)	Mean reduction
20	174	173	170	166	166	1.00
100	135	134	131	128	128	0.77
200	156	155	152	148	148	0.89
300	165	164	161	157	157	0.95
400	146	145	143	139	139	0.84
500	124	123	121	118	118	0.71
600	107	106	105	102	102	0.61
700	88	87	86	84	84	0.51
800	52	52	51	50	50	0.30

The data were obtained from Xiong's experiments

$$N_{\mathrm{pl,Rk}} = A_{\mathrm{s}} f_{\mathrm{y}} + A_{\mathrm{c}} f_{\mathrm{ck}} \tag{4}$$

where A_s and A_c are cross-sectional areas of the steel section, concrete core respectively. f_y and f_{ck} are characteristic strengths of structural steel and concrete core respectively.

To account for overall buckling of the column, the reduction factor χ is given in terms of the relative slenderness $\overline{\lambda}$ and the corresponding buckling curve as follows,

$$\chi = (\Phi + \sqrt{\Phi^2 - \overline{\lambda}^2})^{-1} \leq 1.0 \tag{5}$$

where $\Phi = 0.5\left[1 + \alpha(\overline{\lambda} - 0.2) + \overline{\lambda}^2)\right]$ and

$$\overline{\lambda} = \sqrt{\frac{N_{\mathrm{pl,Rk}}}{N_{\mathrm{cr}}}} \tag{6}$$

α is an imperfection factor corresponding to the appropriate buckling curve. For concrete filled tubes, buckling curve "a" and $\alpha = 0.21$ are adopted if the reinforcement ratio does not exceed 3%. In the tests, there is no reinforcement in the UHSCFST columns, therefore $\alpha = 0.21$ is adopted herein. For comparison with test results, $N_{\mathrm{pl,Rk}}$ calculated from Eq. (4) should be based on characteristic strengths. $N_{cr} = \pi^2 (EI)_{eff} / l_e^2$ is the Euler buckling load of the composite column, and $(EI)_{eff} = E_a I_a + 0.6 E_{cm} I_c$ is the effective flexural stiffness of the composite cross-section, where E_a is the modulus of elasticity of the structural steel and E_{cm} is the secant modulus of elasticity of concrete. I_a and I_c are the second moments of area of the structural steel section and the uncracked concrete section respectively.

The characteristic buckling resistance of composite column subject to compression is given as

$$N_{\mathrm{b,Rk}} = \chi N_{\mathrm{pl,Rk}} \tag{7}$$

4.2 Thermal–Mechanical Analysis

During the thermal stress analysis, the element mesh remains the same as the temperature field analysis without fire protection. But the element type is changed from heat transfer element to thermal mechanical element.

In the thermal–mechanical analysis, a 8-node brick element (C3D8R) is adopted for the UHSC core and a 4-node shell element (S4R) for steel tube. The finite element meshes for the column cross-section is shown in Fig. 5a. The column is simply supported at both ends with the boundary conditions as shown in Fig. 5a.

The observed failure mode of specimen USZ-3 and the predicted failure mode from FEM are shown in Fig. 5b, c. The temperatures, stresses and strains at the centre of each element are assumed to be representative of those of the entire element. Furthermore, it is assumed that the steel and the concrete had the same temperature, t, at the interface (Song et al. 2010). Mesh convergence studies have been performed to study the sensitivity of the mesh size on the predicted results. An optimized mesh size of 20 mm (length):20 mm (width):60 mm (depth) for the part of specimen inside furnace, 20 mm (length):20 mm (width):100 mm (depth) for the rest part of specimen outside furnace was

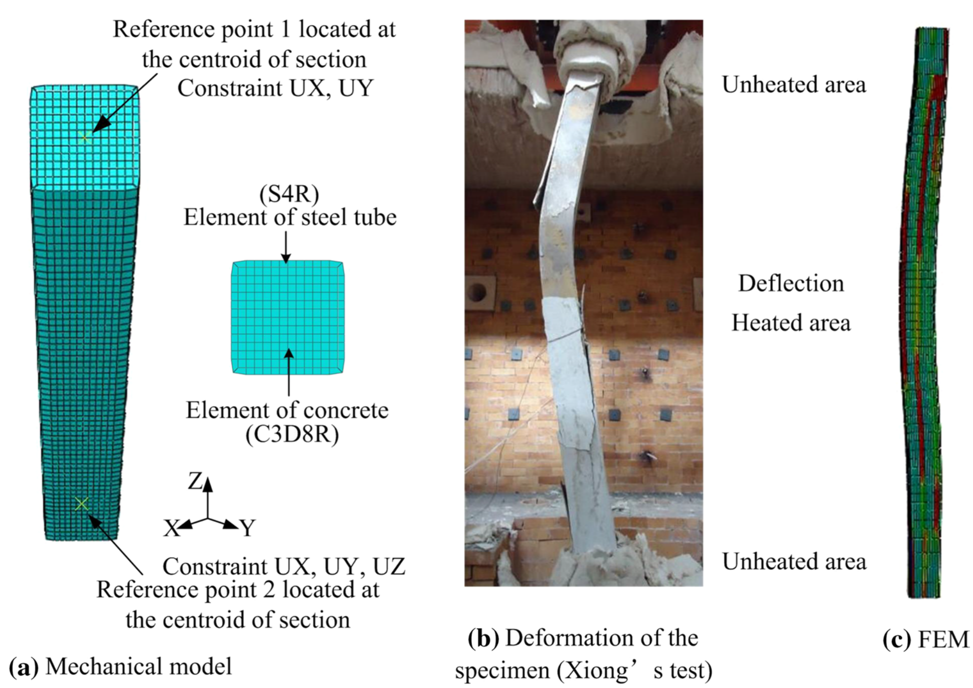

Fig. 5 Boundary conditions for mechanical models and comparison of experimental and numerical deformed shapes after fire exposure for specimen USZ-3

selected to ensure that the predicted results are within 5% error.

The time-dependent thermal–mechanical analysis was performed using ABAQUS, a general nonlinear finite element program. The column is assumed to have an initial bow imperfection approximating a half-sine curve of mid-height magnitude of length//1000. This member imperfection has been adopted based on the first buckling mode shape of pin-ended column subject to axial compression.

The value of friction coefficient $\mu = 0.2$–0.5 is assumed between the steel tube and concrete core (Espinos et al. 2010). The use of $\mu = 0.2$ causes convergence problem near the failure temperature. The use $\mu = 0.3$ is most appropriate as the predicted displacement–time curve is closer to the test result. What's more, as for the friction coefficient in the tangential direction, this factor has little effect on the fire response of composite columns, finally, $\mu = 0.3$ is selected for the friction coefficient in the longitudinal direction. A "Hard" contact formulation is used to capture the contact pressure between the steel tube and the concrete surfaces in the transverse direction. Separation is allowed when the two surfaces move in different direction.

The period of time that a column can maintain the compressive load when subject to the ISO-834 Standard fire is determined (ISO-834-1 1999). For a column member subject to compression, failure occurs when either of the following two criteria is reached:

1. The axial deformation of the column reaches $0.01L$ mm, or
2. The axial deformation velocity exceeds $0.003L$ mm/min, where L is the fire exposed length of column in millimeter.

The results from the numerical analyses and tests are shown in Fig. 6, and the comparisons are given in Table 4. The error of predicting the fire resistance of the concrete filled tubular columns, as compared to the test results, is within 13%. The error is considered to be reasonable and the numerical model will be used for parametric analyses in the subsequent sections.

5 Parametric Study on Factors Influencing Fire Resistance

Parametric analysis is carried out on ultra-high strength concrete filled square tube section with side length a and tube thickness t_s, longitudinal length L, and is subjected to fire. The column is assumed to have an initial bow imperfection approximating a half-sine curve of mid-height magnitude of Length//1000. The column ends are assumed to be simply supported and it is subjected to axial compression. The same failure criteria as described in Sect. 4 are assumed in calculating the fire resistance of the UHSCFST column. The load acting on the column is $0.5N_{b,Ek}$ in which $N_{b,Ek}$ is the characteristic buckling resistance of the member at ambient temperature based on Eurocode 4 (2005) prediction.

Parameters that influence the fire resistance of UHSC filled square steel tubes are studied using the finite element model established in Sect. 4. These parameters include fire protection thickness, load ratio β, strengths of the concrete and steel, relative slenderness ratio $\overline{\lambda}$ steel contribution ratio ($\delta = A_s f_y/(A_s f_y + A_c f_c)$, where the A_s and A_c are the cross-sectional areas of steel tube and concrete core, respectively). The results are shown in Figs. 7, 8, 9, 10, 11 and 12.

In the following, the effect of the various factors that determine the fire resistance of UHSCFST columns will be discussed.

5.1 Effect of Fire Protection Thickness

As shown in Fig. 7a, b, the thickness of fire protection has a great influence on the fire resistance of the composite column. The fire protection thickness t_p is varied from 2 to 12 mm, with the thickness of the steel tube t_s, steel contribution ratio δ and relative slenderness ratio $\overline{\lambda}$ unchanged. The relationship between the increase of fire protection and the fire resistance is almost linear and this information is easy to be used for structural-fire design of concrete filled tube. In the beginning of heating, thermal axial expansion is more serious for columns with thinner fire protection. As the time of fire exposure is getting longer, the column deflects laterally and eventually leads to axial shortening until failure occurs with run-away deflection. Figure 7b shows the relationship between the fire protection thickness and the fire resistant time of the column. The increase of fire resistance time is about 15 min per unit thickness of fire protection in mm. The minimum fire protection thickness is about 5 mm to attain a 2-h ISO standard fire rating.

5.2 Effect of Load Ratio

Figure 8a shows the effects of load ratio on the fire resistance of the composite column, with the thickness of fire protection t_p, steel contribution ratio δ and relative slenderness ratio $\overline{\lambda}$ unchanged. It is apparent that the upward expansion is larger for columns subject to smaller load ratio. Figure 8b shows that the relationship between the fire resistant time and load ratio is linear. With the load ratio increasing, the fire resistance of the column decreases rapidly. As expected, the fire resistance rating of the composite column decreased with an increase of applied load nearly in linear. For example, the fire resistance decreases 8% while the load ratio β changes from 0.3 to 0.4, and this trend is still mild with the value of load ratio increasing. The fire resistance time

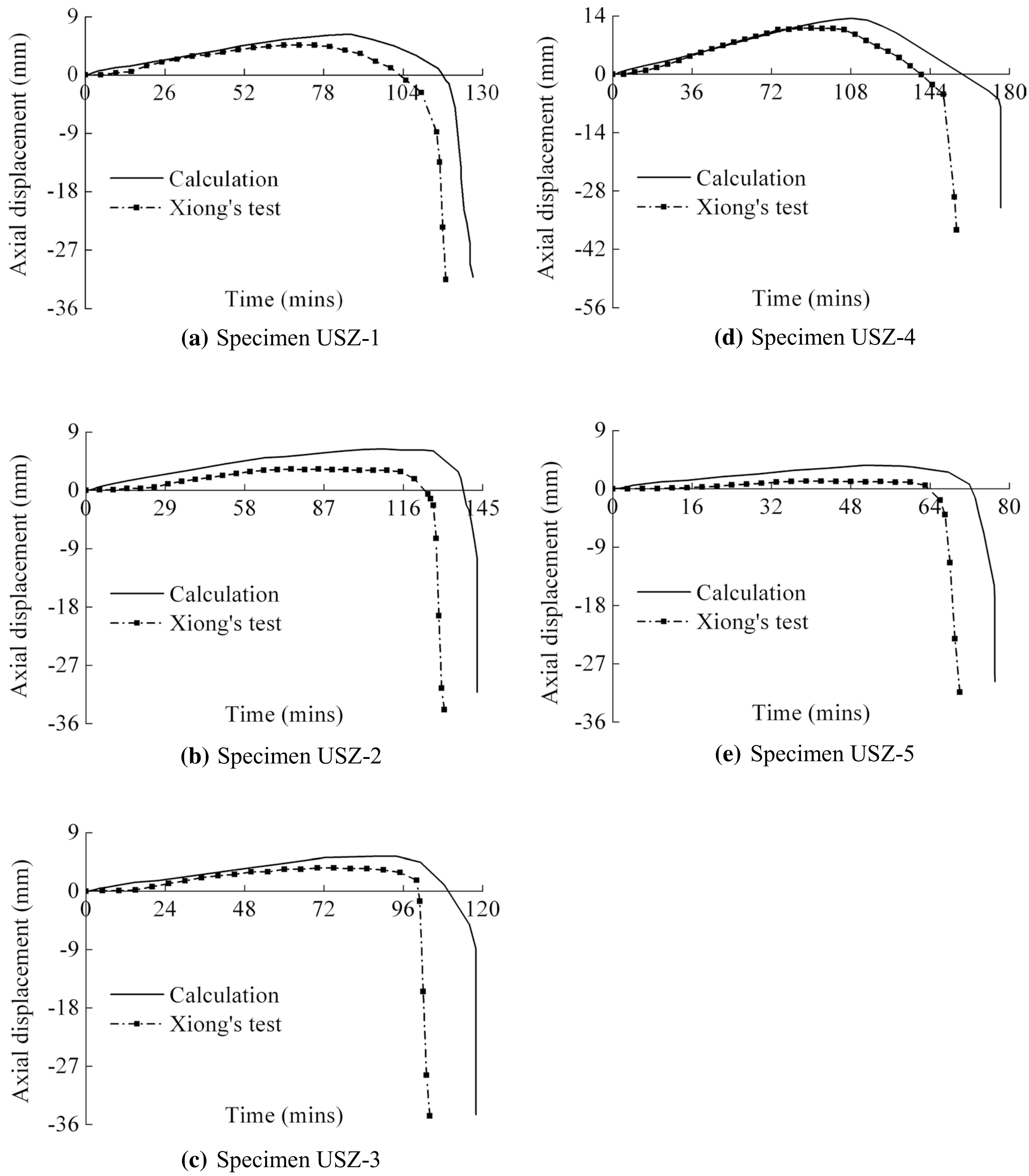

Fig. 6 Comparison of fire resistance between the calculation results and experimental results (Xiong 2013)

decreases only 7% while the load ratio β varies from 0.8 to 0.9.

5.3 Effect of Concrete Strength

The effect of concrete strength was investigated by calculating the fire resistance of the columns for six concrete strengths, namely, 130, 140, 150, 160, 170, and 180 MPa. Figure 9a shows the effects of concrete strength on fire resistance of composite column, with the thickness of fire protection t_p, load ratio β and strength of steel f_y unchanged. Figure 9b plots the fire resistant time with respected to the concrete strength. It shows that the influence of concrete strength on the fire resistance of the composite column is insignificant. For example, the fire resistance increases only 6%, while the concrete strength varies from $f_c = 130$ MPa to $f_c = 180$ MPa, about 38% increment. The fire resistance improves slightly and almost linearly with an increase of the concrete strength.

Table 4 Comparison of fire resistance time between predicted and test results

Specimen	t_p(mm)	β^*	FR*-predicted (min)	FR*-experiment (min)	Error (%)
USZ-1	8.0	0.63	127	118	8
USZ-2	11.5	0.59	143	131	9
USZ-3	9.1	0.47	118	104	13
USZ-4	8.8	0.53	176	156	13
USZ-5	9.5	0.56	77	70	10

"FR" is the fire resistance time. "β" is load ratio

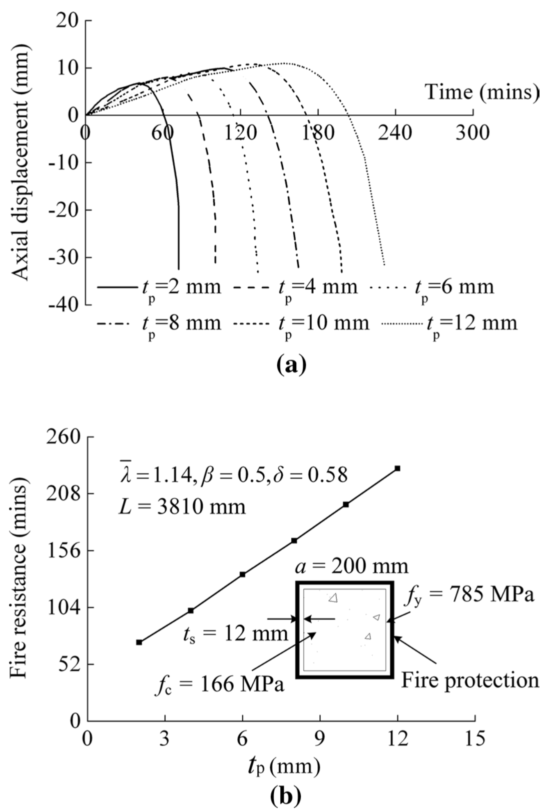

Fig. 7 Relationship between fire protection thickness (mm) and fire resistant time (mins)

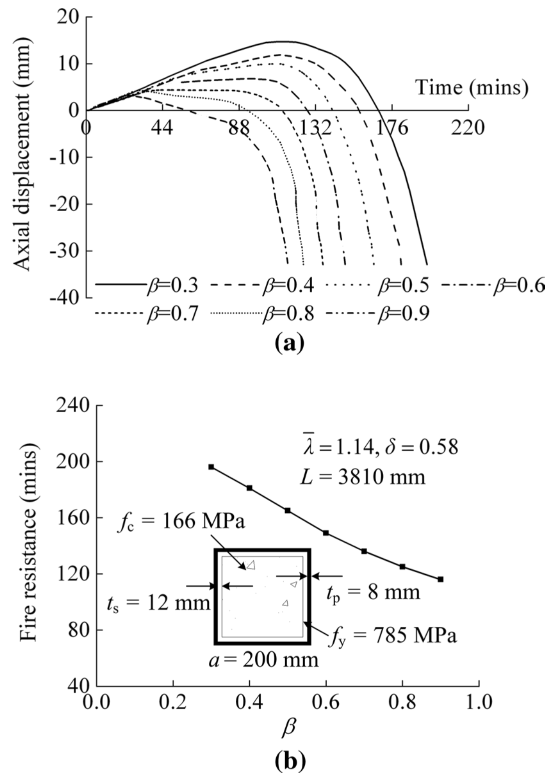

Fig. 8 Relationship between load ratio and fire resistance time (mins)

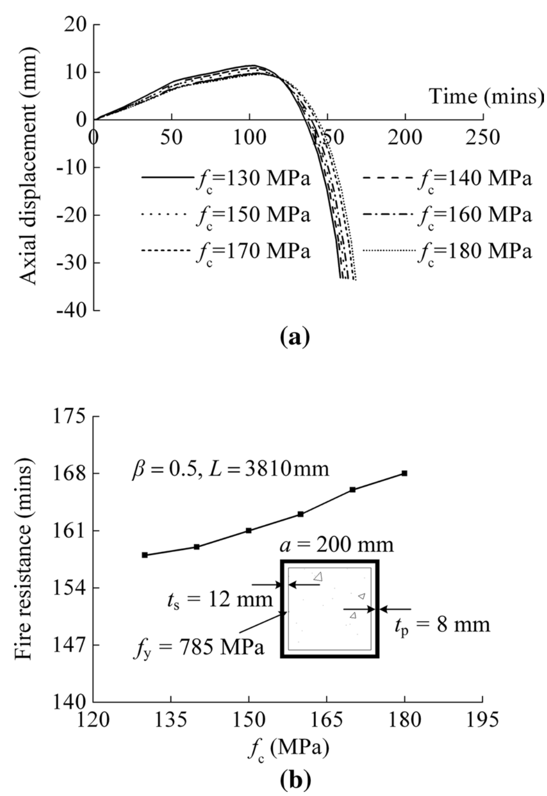

Fig. 9 Relationship between concrete strength (MPa) and fire resistance time (mins)

5.4 Effect of Steel Strength

Figure 10a shows the effects of steel strength on fire resistance of composite column, with the thickness of fire protection t_p, load ratio β and strength of concrete f_c unchanged. Figure 10b shows the fire resistant time with respected to the steel strength. It is observed that the steel strength has a moderate influence on the fire resistance of the composite column. The fire resistance improves slightly but linearly as the steel strength increases. For example, the fire resistance increases only 3%, while the concrete strength varies

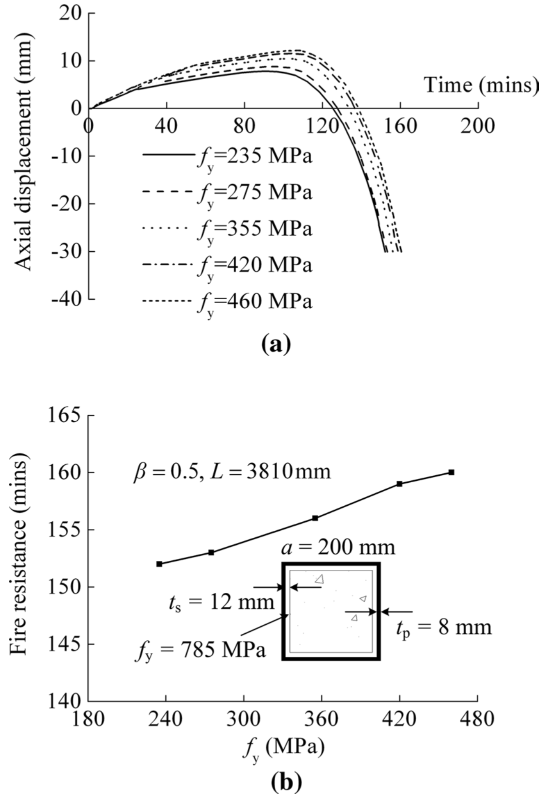

Fig. 10 Relationship between steel strength (MPa) and fire resistance time (mins)

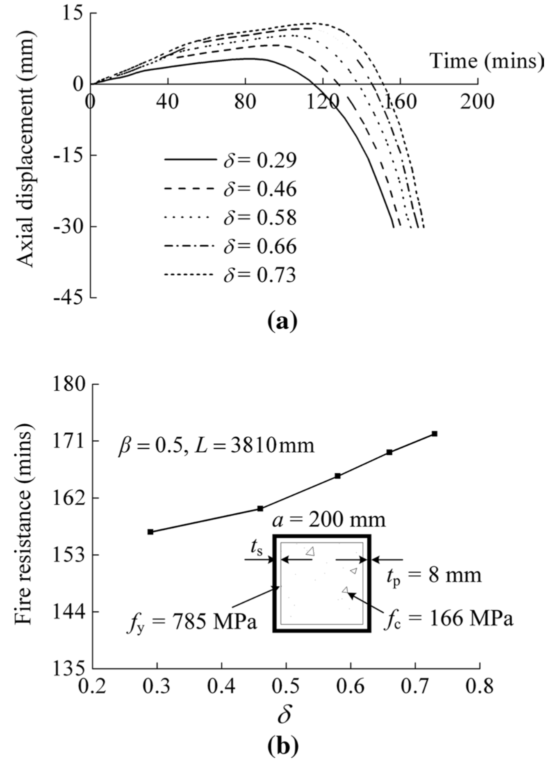

Fig. 11 Relationship between steel contribution ratio and fire resistance time (mins)

from $f_y = 235$ MPa to $f_y = 355$ MPa, about 51% increment. In addition, the fire resistance increases only 1%, while the concrete strength varies from $f_y = 420$ MPa to $f_y = 460$ MPa, about 10% increment.

5.5 Effect of Steel Contribution Ratio

The fire resistance of UHSCFST column increases with the increase of steel contribution ratio as shown in Fig. 11a, b, with the thickness of fire protection t_p, load ratio β, strength of concrete f_c and strength of steel f_y unchanged. The fire resistance of the columns improves slightly with the increase of steel contribution ratio. With the steel ratio varied from 0.29 to 0.46, the fire resistance increases 4 min, in other words, only 2% increment.

5.6 Effect of Relative Slenderness Ratio

It is well known that the slenderness plays an important role in the buckling resistance of a column in compression. In order to study the effect of the column slenderness on fire resistance of UHSCFST column, the relative slenderness ratio $\overline{\lambda}$ varies from 0.38 to 1.52 by changing the column length L from 1270 to 5080 mm with an initial imperfection of L/1000. Figure 12b shows that the relative slenderness ratio has a significant influence on the fire resistance of composite column, with the thickness of fire protection t_p, load ratio β and steel contribution ratio δ unchanged. The fire resistance decreases significantly with the increase of the relative slenderness ratio. This can be attributed to larger second-order moment due to axial force acting on higher lateral deflection of the column with larger relative slenderness ratio.

6 Discussion

The proposed finite element method (FEM) is feasible to calculate fire resistance of UHSCFST columns by using ABAQUS. A full package of heat transfer analysis and coupled thermal–mechanical analysis is needed for each time step and can be achieved. The behaviour of specimens mainly depends on the temperature range as subjected to fire. During the early stages of fire exposure, the steel column carries most of the load. This is because the steel section expands more rapidly the concrete core. At increased temperatures, the steel section yields because of decreasing strength and the column suddenly contracts (Kodur 1998). Figure 7a, b show the thickness of fire protection has a great influence on fire resistance of the composite

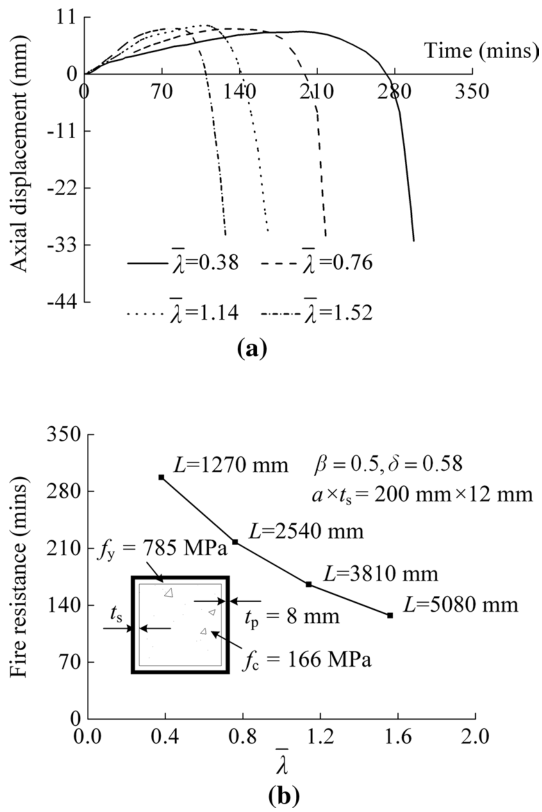

Fig. 12 Relationship between relative slenderness ratio and fire resistance time (mins)

column. Because it can slow down the heating rate of steel and concrete core. The influence of steel contribution ratio, the strength of concrete and steel on fire resistance is unconspicuous, as these factors can not decrease the heating rate of specimens during the fire exposure. The relative slenderness ratio also has significant impact on fire resistance of composite column as shown in Fig. 12a, b. Under the same specimen length and boundary condition, with the specimen cross section size increasing, the speed of temperature rise is slowing down. So the strength of the materials reduces slowly.

Based on the analysis results, the thickness of protection, load ratio, and relative slenderness ratio have significant effects on the fire resistance of UHSCFST columns subject to constant axial load. Whereas, the other parameters, such as the steel contribution ratio, the strength of concrete and steel have only moderate effects on the fire resistance of the columns.

7 Conclusions

In this paper, numerical heat transfer and nonlinear thermal–mechanical analyses are carried out to investigate the behavior and fire resistance of ultra-high strength concrete filled square steel tubular columns under constant axial load. Also the results of the parametric studies on fire resistance of ultra-high strength concrete filled square steel tubular columns are described. The results of the numerical analyses were compared with the available experimental results, and the following conclusions can be drawn:

1. The calculation results of temperature fields are in reasonable agreement with the experimental results and most of the differences within 5%. By considering the influence of friction coefficient in specimen longitudinal direction, the calculation results of displacement–time of the specimens are closer to the test results with an accuracy that is adequate for practical purposes.
2. The temperature distribution of the cross section and the fire resistance of the UHSCFST columns calculated from the proposed numerical model are in reasonable agreement with the experimental results. In some cases, the failure UHSCFST columns by axial compression occurred suddenly, without warning. Based on that above, the numerical models proposed can be used to study the important parameters that will affect the fire resistance of UHSC filled square tubular columns.
3. The material models based on the Eurocode are used to analyze the structural behavior of the UHSCFST columns to gain insight into the failure mechanism. Before attaining the maximum axial deformation, the data of experiment is close to that calculated by numerical model. Compared the calculation results with the experimental results, it indicates that the numerical models can be used to describe the failure of the specimens in the fire test.
4. The fire resistances of UHSCFST columns are evaluated for varying parameters such as the thickness of protection, load ratio, steel contribution ratio, and relative slenderness ratio. The thickness of protection, load ratio, and relative slenderness ratio were found to have significant effects on the fire resistance of UHSCFST columns under axial compression. Whereas the steel contribution ratio, the strength of concrete, and strength of steel were found to have only moderate effects on the fire resistance of the columns, if other parameters were kept the same.

Acknowledgements The research work is financially supported by the National Natural Science Foundation of China (No. 51578134), Research Fund of Shandong Co-Innovation Center for Disaster Prevention and Mitigation of Civil Structures (No. XTP201903), and Doctoral Research Fund of Shandong Jianzhu University (No. XNBS1927). All sources are gratefully acknowledged. The authors are grateful to Professor J. Y. Richard Liew, Department of Civil and Environmental Engineering, National University of Singapore, for his useful comments.

References

Architectural Institute of Japan. (2008). *Recommendations for design and construction of concrete-filled steel tubular structures*. Tokyo: Architectural Institute of Japan.

Choe, G., Kim, G., Gucunski, N., & Lee, S. (2015). Evaluation of the mechanical properties of 200 MPa ultra-high-strength concrete at elevated temperatures and residual strength of column. *Construction and Building Materials, 86*, 159–168.

Chung, K., Park, S., & Choi, S. (2009). Fire resistance of concrete filled square steel tube columns subjected to eccentric axial load. *International Journal of Steel Structures, 9*(1), 69–76.

Chung, K. S., Kim, J. H., & Yoo, J. H. (2013). Experimental and analytical investigation of high-strength concrete-filled steel tube square columns subjected to flexural loading. *Steel Composite Structures, 14*(2), 133–153.

Dai, X. H., & Lam, D. (2012). Shape effect on the behaviour of axially loaded concrete filled steel tubular stub columns at elevated temperature. *Journal of Constructional Steel Research, 73*, 117–127.

ECCS-Technical Committee 3. (1988).*Fire safety of steel structures, technical note, calculation of the fire resistance of centrally loaded composite steel-columns exposed to the standard fire*.

ECS, Eurocode 2. (2004).*Design of concrete structures-part 1–2, general rules-structural fire design*, EN 1992-1-2. European Committee for Standardization.

ECS, Eurocode 3. (2005).*Design of steel structures-part 1–2, general rules-structural fire design*, EN 1993-1-2. European Committee for Standardization.

ECS, Eurocode 4. (2005).*Design of composite steel and concrete structures-part 1–2, general rules-structural fire design*, EN 1994-1-2. European Committee for Standardization.

Espinos, A., Romero, M. L., & Hospitaler, A. (2010). Advanced model for predicting the fire response of concrete filled tubular columns. *Journal of Constructional Steel Research, 66*, 1030–1046.

Fong, M., Chan, S. L., & Uy, B. (2011). Advanced design for trusses of steel and concrete-filled tubular sections. *Engineering Structures, 33*(12), 3162–3171.

Han, L. H., Yang, Y. F., & Xu, L. (2003). An experimental study and calculation on the fire resistance of concrete-filled SHS and RHS columns. *Journal of Constructional Steel Research, 59*(4), 427–452.

Hassanein, M. F., Kharoob, O. F., & Gardner, L. (2015). Behaviour and design of square concrete-filled double skin tubular columns with inner circular tubes. *Engineering Structures, 100*, 410–424.

ISO-834-1. (1999).*Fire-resistance tests-elements of building construction part 1: General requirements*. Geneva: International Standard ISO-834.

Jamaluddin, N., Lam, D., Dai, X. H., & Ye, J. (2013). An experimental study on elliptical concrete filled columns under axial compression. *Journal of Constructional Steel Research, 87*, 6–16.

Kodur, V. K. R. (1998). Performance of high strength concrete-filled steel columns exposed to fire. *Canadian Journal of Civil Engineering, 25*, 975–981.

Lee, J. H., Sohn, Y. S., & Lee, S. H. (2012). Fire resistance of hybrid fibre-reinforced, ultra-high-strength concrete columns with compressive strength from 120 to 200 MPa. *Magazine of Concrete Research, 64*(6), 539–550.

Lie, T. T. (1992). *Structural fire protection. Manuals and reports on engineering practice* (Vol. 78). New York: ASCE.

Liew, J. Y. R., Xiong, M. X., & Tran, C. T. (2015). *Design guide for concrete filled tubular members with high strength materials—An extension of Eurocode 4 method to C90/105 concrete and S550 steel* (pp. 23–40). Singapore: Building and Construction Authority of Singapore.

Liew, J. Y. R., Xiong, M. X., & Xiong, D. X. (2014). Design of high strength concrete filled tubular columns for tall buildings. *International Journal of High-Rise Buildings, 3*(3), 1–7.

Lyu, X., Shu, G. P., Liew, J. Y. R., & Du, E. F. (2018). Fire resistance of steel tubular columns infilled with ultra-high strength concrete. *Advanced Steel Construction, 14*(3), 438–460.

Mao, X. Y., & Kodur, V. K. R. (2011). Fire resistance of concrete encased steel columns under 3- and 4-side standard heating. *Journal of Constructional Steel Research, 67*, 270–280.

Park, S. H., Choi, S. M., & Chung, K. S. (2008). A study on the fire-resistance of concrete-filled steel square tube columns without fire protection under constant central axial loads. *Steel and Composite Structures, 8*(6), 491–510.

Qu, X. S., Chen, Z. H., & Sun, G. J. (2015). Axial behaviour of rectangular concrete-filled cold-formed steel tubular columns with different loading methods. *Steel and Composite Structures, 18*(1), 71–90.

Rush, D., Bisby, L., Jowsey, A., Melandinos, A., & Lane, B. (2012). Structural performance of unprotected concrete-filled steel hollow section in fire: A review and meta-analysis of available test data. *Steel and Composite Structures, 12*(4), 325–352.

Shin, H. O., Yoon, Y. S., Cook, W. D., & Mitchell, D. (2015). Effect of confinement on the axial load response of ultrahigh-strength concrete columns. *Journal of Structural Engineering, 141*(6), 04014151.

Shu, G. P., & Lv, X. (2013). Ultimate bearing capacity factor and whole process analysis for large size concrete filled steel tube columns. *The IES Journal Part A: Civil and Structural Engineering, 6*(2), 165–172.

Song, T. Y., Han, L. H., & Uy, B. (2010). Performance of CFST column to steel beam joints subjected to simulated fire including the cooling phase. *Journal of Constructional Steel Research, 66*, 591–604.

Wang, K., & Young, B. (2013). Fire resistance of concrete-filled high strength steel tubular columns. *Thin-Walled Structures, 71*, 46–56.

Xiao, J. Z., Li, Z. W., Xie, Q. H., & Shen, L. M. (2016). Effect of strain rate on compressive behaviour of high-strength concrete after exposure to elevated temperatures. *Fire Safety Journal, 83*, 25–37.

Xiong,M. X. (2013). *Fire resistance of ultra-high strength concrete filled steel tubular columns*. Ph.D. Dissertation, National University of Singapore, Singapore.

Xiong, M. X., & Liew, J. Y. R. (2016). Mechanical behaviour of ultra-high strength concrete at elevated temperatures and fire resistance of ultra-high strength concrete filled steel tubes. *Materials & Design, 104*, 414–427.

Yu, M., Zha, X. X., Ye, J. Q., & Li, Y. (2010). Fire responses and resistance of concrete-filled steel tubular frame structures. *International Journal of Structural Stability and Dynamics, 10*(2), 253–271.